공학석사학위논문

영구자석 전동기 권선 단락 고장 진단을 위한 추정 외란 신호 분리 기법

Estimated Disturbance Decomposition Based Fault Detection for Inter-Turn Short-Circuit Fault in PMSM

2020 년 2 월

서울대학교 대학원

기계항공공학부

안 길 준

Abstract

Estimated Disturbance Decomposition Based Fault Detection for Inter-Turn Short-Circuit Fault in PMSM

Giljun Ahn
Department of Mechanical and Aerospace Engineering
The Graduate School
Seoul National University

This paper proposes a robust and simple to implement method for detecting inter-turn short-circuit faults of surface-mounted permanent magnet synchronous motors (SPMSMs) based on the estimated disturbance. The total disturbance of motor with inter-turn short-circuit fault includes disturbance from several sources such as parameter variations, unmodeled dynamics and fault. The proposed method consists of three steps. First, the disturbance is estimated using disturbance observer (DBO). Second, the estimated disturbance is separated into faulty disturbance and healthy disturbance. The healthy disturbance consists of effects from parameter variations and unmodeled dynamics such as noise. Third, a new fault indicator is calculated which has a relationship with the fault severity and able to estimate the fault severity. The simulation results verify the effectiveness of the proposed method with steady state response and transient response. And these verify the robustness with parameter variations and noise. The proposed method can detect inter-turn short-circuit faults without additional sensors under uncertainties. This strength can facilitate on-line fault detection in industrial field applications.

Keywords: Disturbance observer
Fault diagnosis
Inter-turn short-circuit fault
Permanent magnet synchronous motor

Student Number: 2018-22822

Table of Contents

List of Tables

List of Figures

Nomenclatures

$\mathbf{v}_{abc}$	Stator voltage vector of abc-reference frame
$\mathbf{i}_{abc}$	Stator current vector of abc-reference frame
$\mathbf{\Psi}_{abc}$	Flux linkage vector of permanent magnet of abc-reference frame
$\mathbf{v}_0$	Voltage vector of neutral point
$\mathbf{R}_s$	Resistance matrix of abc-reference frame
$\mathbf{L}_s$	Inductance matrix of abc-reference frame
μ	Ratio of the number of shorted turns to normal turns
R_f	Resistance of short circuit
S	Fault severity
ω_e	Electrical angular velocity
$\mathbf{T}_{abc}^{dq0}$	Park's transformation matrix
$\mathbf{v}_{dq0}$	Stator voltage vector of dq-reference frame
$\mathbf{i}_{dq0}$	Stator current vector of dq-reference frame
$\mathbf{v}_{dqh}$	Healthy voltage vector of dq-reference frame
$\mathbf{v}_{dqf}$	Faulty voltage vector of dq-reference frame
$\boldsymbol{\delta}_{dq}$	Lumped disturbance vector of dq-reference frame
$\boldsymbol{\epsilon}_{dq}$	Disturbance vector of dq-reference frame caused by unmodeled dynamics
$\mathbf{f}_{dq}$	Disturbance vector of dq-reference frame caused by inter-turn short-circuit fault

Chapter 1. Introduction

1.1 Motivation

Permanent magnet synchronous motors (PMSMs) are widely used in various field requiring high precision and high torque control systems, such as industrial robots. Because the PMSMs are main component of overall industry, an unexpected failure of the PMSM may cause a large financial loss [1].

The major failure components of the motor are bearing, stator and rotor. The failures of rotor mostly occur in induction motors. The table1 shows the percentage of motor failure components [2]. The stator winding fault accounts for 36% of electric machine failures [2-4]. There are several types of stator winding fault and the inter-turn short-circuit fault (ISCF) is the initial fault of stator winding. ISCF is caused by failure of winding insulation. The winding insulation is degraded by combination of thermal, mechanical and electrical stresses. The electrical stress from pulse width modulation (PWM) inverter makes the ISCFs more prevalent [5]. Thus, the early fault detection of ISCF in PMSMs before the fault becomes fatal is important to prevent the enormous loss.

Various methods to detect the ISCF in electric machines have been proposed. Motor current signature analysis (MCSA) is the most common method based on monitoring of the motor current harmonics and sideband of the characteristic frequencies around the supply frequency [6-8]. But the harmonics are sensitive to the motor drive and can be overlapped by harmonics of other fault modes [9]. These hurt the robustness of fault detection using MCSA. Zero sequence voltage component (ZSVC) method was developed to detect the ISCF in early stage [1, 10]. But ZSVC

method has several disadvantages. This method is invasive because it requires an access to the neutral point. An external resistor network is required to decouple the ZSVC from the inverter effect [11]. Because of the external resistor network, ZSVC is not appropriate for several applications with complex operating environment such as industrial robots and machining tools. There are developed method based on signal processing with vibration, acoustic and flux sensors. Though the methods with external sensors show good performance for detect faults, they are not appropriate for complex operating environments like ZSVC mentioned above. In [12], improvement of ISCF detection technique using high frequency signal injection to control voltages is presented. However, high frequency injection method causes additional electromagnetic noise and acoustic noise [13]. There are state observer-based methods using such as sliding mode observer, extended state observer and kalman filter have been devised. [14] calculates residual between measured and estimated stator currents using high-order sliding mode observer to detect ISCF. But this method overlooks parameter variations and unmodeled dynamics in healthy machines which hamper the robustness of ISCF detection.

In summary, this thesis deals with ISCF of PMSM and proposes an improved method to diagnose ISCF of PMSM in early stage without the disadvantages of the aforementioned developed methods.

Table 1 Percentage of motor failure components

Failure component	Percentages
Bearing	41 %
Stator	36 %
Rotor	9 %
Others	14 %

1.2 Scope of Research

This thesis proposes an improved method to diagnose ISCF of PMSM in early stage. The main contributions of the proposed method are as below.

1) The proposed method does not require the additional equipment.
2) The proposed method is robust against the parameter variations and unmodeled dynamics.
3) The proposed method prevents the false alarm and eliminate the effect of rotating speed.

The proposed method based on mathematical model of PMSM with ISCF does not require additional sensors or accessible neutral point. To improve the robustness, the proposed method takes account of the uncertainties from unmodeled dynamics and parameter variations from the operating conditions using disturbance observer (DBO). The total estimated disturbance by DBO and disturbance caused by ISCF is identified mathematically. The disturbance from fault is decomposed from the estimated disturbance to diagnose the ISCF. Finally, using the decomposed disturbance, a new fault indicator to prevent false alarm and eliminate the effect of

rotating speed is proposed in this thesis.

1.3 Thesis Layout

This thesis consists of five chapters. The chapter 2 addresses the mathematical model and the disturbances of PMSM with ISCF which is the background of this research. And the chapter 3 describes the proposed method; Estimated disturbance decomposition method. Then, the chapter 4 represents the simulation results which validate the efficiency and robustness of the proposed method. Lastly, the conclusion is presented in the chapter 5.

Chapter 2. Background

The chapter 2 describes the mathematical model of PMSM with ISCF at section 2.1 and its disturbance analysis at section 2.2.

2.1 Mathematical Model of Faulty PMSM

Figure 2-1 shows 3-phase PMSM which has an inter-turn short-circuit fault with shorted turn ratio $\mu = N_2/(N_1+N_2)$ at phase a. N_1 and N_2 are the number of healthy turns and shorted turns. R_f is the resistance which models the stator winding insulation failure and i_f is the current of shorted circuit. This is one of the most widely used short-circuit fault model. The voltage equation in abc-reference frame of PMSM with inter-turn short-circuit fault is expressed as [15]:

$$\mathbf{v}_{abc} = \mathbf{R}_s\mathbf{i}_{abc} + \mathbf{L}_s\frac{d}{dt}(\mathbf{i}_{abc}) + \frac{d}{dt}(\mathbf{\Psi}_{fabc}) + \mathbf{v_0} \tag{2.1}$$

where $\mathbf{v}_{abc}$, $\mathbf{i}_{abc}$ and $\mathbf{v}_0$ are the stator voltage vector, stator current vector and zero-sequence voltage vector. $\mathbf{R}_s$, $\mathbf{L}_s$ and $\mathbf{\Psi}_{abc}$ are the stator resistance matrix, inductance matrix and flux linkage matrix due to permanent magnet.

$$\begin{bmatrix} v_a \\ v_b \\ v_c \\ 0 \end{bmatrix} = \begin{bmatrix} R_s & 0 & 0 & -\mu R_s \\ 0 & R_s & 0 & 0 \\ 0 & 0 & R_s & 0 \\ \mu R_s & 0 & 0 & -\mu R_s - R_f \end{bmatrix} \begin{bmatrix} i_a \\ i_b \\ i_c \\ i_f \end{bmatrix} + \begin{bmatrix} L & M & M & -\mu L \\ M & L & M & -\mu M \\ M & M & L & -\mu M \\ \mu L & \mu M & \mu M & -\mu^2 L \end{bmatrix} \frac{d}{dt} \begin{bmatrix} i_a \\ i_b \\ i_c \\ i_f \end{bmatrix} + \frac{d}{dt} \begin{bmatrix} \psi_a \\ \psi_b \\ \psi_c \\ \psi_f \end{bmatrix} + v_0 \begin{bmatrix} 1 \\ 1 \\ 1 \\ 0 \end{bmatrix} \tag{2.2}$$

$$\begin{cases} \psi_a = \psi_{PM,1}\, cos(\theta_e) + \sum_{v=2k+1} \psi_{PM,v}\, cos\, v(\theta_e - \theta_v) \\ \psi_b = \psi_{PM,1} cos\left(\theta_e - \frac{2\pi}{3}\right) + \sum_{v=2k+1} \psi_{PM,v}\, cos\, v\left(\theta_e - \theta_v - \frac{2\pi}{3}\right) \\ \psi_c = \psi_{PM,1} cos\left(\theta_e + \frac{2\pi}{3}\right) + \sum_{v=2k+1} \psi_{PM,v}\, cos\, v\left(\theta_e - \theta_v + \frac{2\pi}{3}\right) \\ \psi_f = \mu\left\{\psi_{PM,1}\, cos(\theta_e) + \sum_{v=2k+1} \psi_{PM,v}\, cos\, v(\theta_e - \theta_v)\right\} \end{cases} \quad (2.3)$$

R_s is the stator resistance, and L and M are self and mutual inductance. ω_e is electrical angular velocity and θ_e is electrical angle. flux linkage matrix $\mathbf{\Psi}_{abc}$ includes the *n*th harmonics components as shown in (2.3) which can be ignored because those amplitudes are small enough compared to that of fundamental component $\psi_{PM,1}$. And ψ_f is the faulty term of flux of permanent magnet. Therefore, only the fundamental components are considered except the harmonics in this paper. The last row of (2.2) which expresses the short-circuit of short-circuit is as below where L_s is *L*-*M*.

$$0 = \mu R_s i_a + \mu L_s \frac{di_a}{dt} - (\mu R_s + R_f) i_f - \mu^2 L \frac{di_f}{dt} + \frac{d}{dt}(\mu \psi_f cos\theta) \quad (2.4)$$

If μ is small enough, which means that the fault severity is mild, (2.4) can be rewritten as:

$$i_f \approx \mathrm{I_f} \sin(\theta + \theta_f) \quad (2.5)$$

Where

$$\begin{cases} I_f = \dfrac{\mu}{R_f + \mu R_s}\sqrt{(R_s^2 + \omega_e^2 L_s^2) I_a^2 + \psi_f^2 \omega_e^2} \\ \theta_f = tan^{-1}\left(\dfrac{L_s \omega_e I_a}{R_s I_a - \omega_e \psi_f}\right) \end{cases} \tag{2.6}$$

Fault current i_f can be expressed as (2.7) because the last term of (2.4) is a dominant term and the phase with short-circuit is *a* phase [15]. Hence, the amplitude of fault current I_f is proportional to fault severity $S = \mu/(R_f + \mu R_s)$ and electrical rotating speed ω_e.

$$i_f \approx I_f \, sin\big(\theta_e + \theta_f\big) = k_1 S \omega_e \, sin\big(\theta_e + \theta_f\big) \tag{2.7}$$

The abc to dq0 transformation matrix is defined as:

$$\mathbf{T}_{abc}^{dq0} = \frac{2}{3}\begin{bmatrix} cos(\theta_e) & cos\left(\theta_e - \dfrac{2\pi}{3}\right) & cos\left(\theta_e + \dfrac{2\pi}{3}\right) \\ sin(\theta_e) & sin\left(\theta_e - \dfrac{2\pi}{3}\right) & sin\left(\theta_e + \dfrac{2\pi}{3}\right) \\ 1/2 & 1/2 & 1/2 \end{bmatrix} \tag{2.8}$$

Applying dq0 transformation to the first three rows of (2.1) results in the voltage equation in dq0 reference frame as (2.9). Except for the last row of (2.9), there is dq-voltage equation as (2.10).

$$\begin{aligned} \mathbf{v}_{dq0} = {} & \mathbf{T}_{abc}^{dq0} R_s \big(\mathbf{T}_{abc}^{dq0}\big)^{-1} \mathbf{i}_{s,dq0} - \mathbf{T}_{abc}^{dq0} \begin{bmatrix} \mu R_s i_f \\ 0 \\ 0 \end{bmatrix} \\ & + \mathbf{T}_{abc}^{dq0} \mathbf{L}_s \frac{d}{dt}\Big(\big(\mathbf{T}_{abc}^{dq0}\big)^{-1} \mathbf{i}_{s,dq0}\Big) - \mathbf{T}_{abc}^{dq0} \begin{bmatrix} \mu L \\ \mu M \\ \mu M \end{bmatrix} \frac{di_f}{dt} \\ & + \mathbf{T}_{abc}^{dq0} \boldsymbol{\Psi}_{fabc} \end{aligned} \tag{2.9}$$

$$\begin{bmatrix} v_d \\ v_q \end{bmatrix} = \begin{bmatrix} R_s & 0 \\ 0 & R_s \end{bmatrix} \begin{bmatrix} i_d \\ i_q \end{bmatrix} + \begin{bmatrix} L_s & 0 \\ 0 & L_s \end{bmatrix} \frac{d}{dt} \begin{bmatrix} i_d \\ i_q \end{bmatrix} + \begin{bmatrix} 0 & -\omega_e \\ \omega_e & 0 \end{bmatrix} (L - M) \begin{bmatrix} i_d \\ i_q \end{bmatrix}$$

$$+ \begin{bmatrix} 0 \\ \omega_e \psi_f \end{bmatrix} + \left\{ -\boldsymbol{T}_{abc}^{dq0} \begin{bmatrix} \mu R_s \\ 0 \\ 0 \end{bmatrix} i_f - \boldsymbol{T}_{abc}^{dq0} \begin{bmatrix} \mu L \\ \mu M \\ \mu M \end{bmatrix} \frac{d i_f}{dt} \right\} \tag{2.10}$$

$$= \mathbf{v}_{dqh} + \mathbf{v}_{dqf}$$

Equation (2.10) represents the dq-voltages PMSM with an inter-turn short-circuit fault composed of a healthy dq-voltage $\mathbf{v}_{dqh}$ and a faulty dq-voltage $\mathbf{v}_{dqf}$.

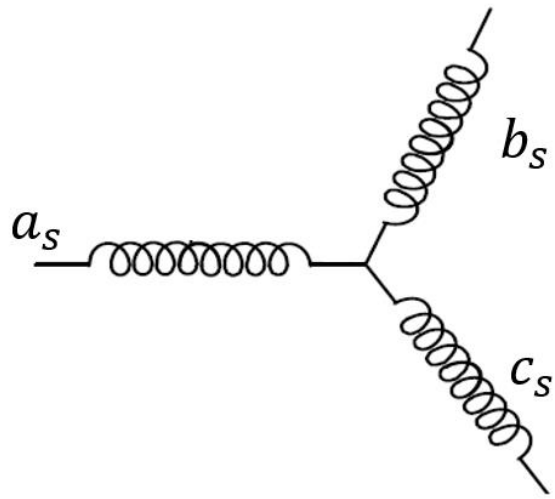

Figure 2-1 Schematic diagram of 3-phase PMSM

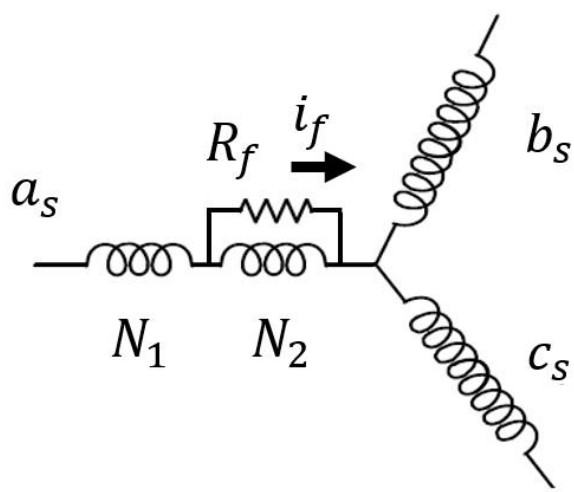

Figure 2-2 Schematic diagram of 3-phase PMSM with stator winding inter-turn short-circuit fault

2.2 Disturbance Analysis of Faulty PMSM

Not only faulty machine but also normal machine has disturbances from various sources such as parameter variations and noise. To know the exact values of parameters of PMSM is difficult because electric machine parameters vary depending on the operating condition and there would be other uncertainties due to unmodeled dynamics [16-18]. Moreover, when the fault occurs on the PMSM, there should be additional disturbances. The voltage equation at *dq*-reference frame of PMSM with disturbance caused by parameter variations, noise and fault is expressed as:

$$\begin{bmatrix} v_d \\ v_q \end{bmatrix} = \begin{bmatrix} R_s + pL_{sn} & -\omega_e L_{sn} \\ \omega_e L_{sn} & R_s + pL_{sn} \end{bmatrix} \begin{bmatrix} i_d \\ i_q \end{bmatrix} + \begin{bmatrix} \delta_d \\ \omega_e \psi_{PM} + \delta_q \end{bmatrix} \tag{2.11}$$

$$\begin{bmatrix} \delta_d \\ \delta_q \end{bmatrix} = \left\{ \begin{bmatrix} \Delta R_s + p\Delta L_s & -\omega_e \Delta L_s \\ \omega_e \Delta L_s & \Delta R_s + p\Delta L_s \end{bmatrix} \begin{bmatrix} i_d \\ i_q \end{bmatrix} + \begin{bmatrix} 0 \\ \omega_e \Delta \psi_{PM} \end{bmatrix} \right\} + \begin{bmatrix} \epsilon_d \\ \epsilon_q \end{bmatrix} + \begin{bmatrix} f_d \\ f_q \end{bmatrix} \tag{2.12}$$

where $\boldsymbol{\delta}_{dq}$ are the lumped disturbance consists of disturbance caused by parameter variations, unmodeled dynamics $\boldsymbol{\varepsilon}_{dq,}$ and inter-turn short-circuit fault $\mathbf{f}_{dq}$. The subscript 'n' and Δ represent nominal parameter values and parameter variations respectively; $R_s = R_{sn} + \Delta R_s,\ L_s = L_{sn} + \Delta L_s,\ \psi_{PM} = \psi_{PMn} + \Delta\psi_{PM}$

According to the equation (2.10) to (2.12), the disturbance due to inter-turn short-circuit fault $\mathbf{f}_{dq}$ can be expressed as below.

$$\begin{bmatrix} f_d \\ f_q \end{bmatrix} = \mathbf{T}_{abc}^{dq0} \left(- \begin{bmatrix} \mu R_{sn} \\ 0 \\ 0 \end{bmatrix} - \begin{bmatrix} \mu L_n \\ \mu M_n \\ \mu M_n \end{bmatrix} \frac{di_f}{dt} \right) \tag{2.13}$$

From equation (2.13), it is clear that the faulty disturbance $\mathbf{f}_{dq}$ is equal to the faulty voltage in *dq*-reference frame $\mathbf{v}_{dqf}$ in (2.10). Therefore, if the faulty disturbance can be estimated, the inter-turn short-circuit fault of the machine can be diagnosed.

Chapter 3. Proposed Method for Diagnosis of Faulty PMSM

This chapter describes the proposed method using estimated disturbance decomposition to diagnose the inter-turn short-circuit fault of PMSM. The proposed method consists of three steps. Each section describes each step of proposed method. Section 3.1 shows the first step, design of disturbance observer to estimate the disturbance. Section 3.2 explains the next step, decomposition of the estimated disturbance. And the last step, calculation of new fault indicator, is shown at section 3.3.

3.1 Disturbance Observer Design

To implement the disturbance observer for fault diagnosis in discrete time, a disturbance observer can be designed as below.

$$\hat{\mathbf{i}}_{dq}(k) = \mathbf{A}\hat{\mathbf{i}}_{dq}(k-1) + \mathbf{B}\left\{\mathbf{v}_{dq}(k-1) + \begin{bmatrix} 0 \\ \omega_e \psi_{sn} \end{bmatrix} - \hat{\boldsymbol{\delta}}_{dq}(k-1)\right\} \tag{3.1}$$

Where

$$\begin{aligned} \mathbf{v}_{dq} &= [v_d(k) \quad v_q(k)]^T \\ \hat{\mathbf{i}}_{dq}(k) &= [\hat{\imath}_d \quad \hat{\imath}_q]^T \\ \hat{\mathbf{f}}_{dq}(k) &= \left[\hat{f}_q(k) \quad \hat{f}_q(k)\right]^T \\ \mathbf{A} &= \begin{bmatrix} 1 - T_s R_{sn}/L_{sn} & 0 \\ 0 & 1 - T_s R_{sn}/L_{sn} \end{bmatrix} \end{aligned} \tag{3.2}$$

$$\mathbf{B} = \begin{bmatrix} T_s/L_{sn} & 0 \\ 0 & 1 - T_s R_{sn}/L_{sn} \end{bmatrix}$$

k represents iteration sample integer and T_s is the sampling period of disturbance observer. The error vector and squared error function of the observer are defined as (3.3) and (3.4).

$$\mathbf{e}(k) = \begin{bmatrix} i_d(k) - \hat{\imath}_d(k) \\ i_q(k) - \hat{\imath}_q(k) \end{bmatrix}^T \tag{3.3}$$

$$\mathbf{E}(k) = \begin{bmatrix} \left(i_d(k) - \hat{\imath}_d(k)\right)^2 \\ \left(i_q(k) - \hat{\imath}_q(k)\right)^2 \end{bmatrix}^T \tag{3.4}$$

[17] adopted a simple steepest descent algorithm too minimize the error function. Jacobian of the error function is calculated in (3.5) for the steepest descent algorithm.

$$\mathbf{J} = \frac{\partial \mathbf{E}(k)}{\partial \widehat{\boldsymbol{\delta}}_{dq}(k)} = \mathbf{B}\mathbf{e}(k) \tag{3.5}$$

Let $\boldsymbol{\gamma} = \mathrm{diag}(\gamma_d, \gamma_q)$ be iterative step-size gain matrix and then, minimizing $\mathbf{E}(k)$ gives following equation which is derived from the gradient search.

$$\begin{aligned} \widehat{\boldsymbol{\delta}}_{dq}(k) &= \widehat{\boldsymbol{\delta}}_{dq}(k-1) + \Delta\widehat{\boldsymbol{\delta}}_{dq}(k-1) \\ &= \widehat{\boldsymbol{\delta}}_{dq}(k-1) - \boldsymbol{\gamma}\mathbf{I}_{2\mathrm{x}2}\mathbf{B}\mathbf{e}(k) \end{aligned} \tag{3.6}$$

3.2 Estimated Disturbance Decomposition

The disturbance caused by inter-turn short-circuit fault in (2.13) can be extended as follows:

$$\begin{bmatrix} f_d \\ f_q \end{bmatrix} = \frac{1}{3}\mu I_f \begin{bmatrix} -R_s\, cos(\theta_f) + L_s\omega_e\, sin(\theta_f) \\ R_s\, sin(\theta_f) + L_s\omega_e\, cos(\theta_f) \end{bmatrix} + \frac{1}{3}\mu I_f \begin{bmatrix} -R_s\, cos(2\theta_e + \theta_f) + L_s\omega_e\, sin(2\theta_e + \theta_f) \\ R_s\, s\, in(2\theta_e + \theta_f) + L_s\omega_e\, cos(2\theta_e + \theta_f) \end{bmatrix} \tag{3.7}$$

It consists of DC and second harmonic component. The lumped disturbance except faulty disturbance includes DC and other components from parameter variations and uncertainties. Therefore, the DC component of lumped disturbance is summation of various sources and not appropriate to detect the fault. On the other hand, the second harmonic component is affected by only the fault of PMSM. The amplitudes of second harmonic component are proportional to μI_f.

$$\mathbf{f}_{dq}(2\theta_e) = \frac{1}{3}\mu I_f \sqrt{R_s^2 + L_s^2\omega_e^2} \begin{bmatrix} \sin(2\theta_e + \alpha) \\ \cos(2\theta_e + \beta) \end{bmatrix} \tag{3.8}$$

Hence, the second harmonic is available to detect the inter-turn short-circuit fault. This paper adopts a band-pass filter (BPF) to decompose the second harmonic component from lumped disturbance.

3.3 Fault Indicator

The second harmonic disturbance decomposed from (2.12) with BPF can be written as below.

$$BPF(\boldsymbol{\delta}_{dq}) = \frac{1}{3}\mu I_f \sqrt{R_s^2 + L_s^2\omega_e^2} \begin{bmatrix} \sin(2\theta_e + \alpha) \\ \cos(2\theta_e + \beta) \end{bmatrix} + \eta \tag{3.9}$$

Its' amplitude is proportional to ω_e^2 when the rotating speed is fast enough. To improve estimation performance, the step size of DBO γ is set to a varying value that is proportional to ω_e^2.

If using only the amplitude of each second harmonic disturbance in d and q axis for fault diagnosis, it may cause false alarm because there would be remaining undesired unknown second harmonic disturbance η due to unmodeled dynamics such as noise. Also since it is proportional to square of rotating speed, it is not suitable for diagnosing faults for various speed conditions. To prevent the false alarm and lessen the effect of the rotating speed, a fault indicator (FI) is proposed in this paper; as root sum squared of each d and q axis band-pass filtered disturbance divided by square of rotating speed (3.10).

$$FI = \frac{\sqrt{\left(BPF(\delta_d)\right)^2 + \left(BPF(\delta_q)\right)^2}}{\omega_e^2} \approx k\mu S \tag{3.10}$$

The DC offset of the fault indicator directly indicates the fault severity. Therefore, a moving average filter (MAF) is used on fault indicator to extract the DC offset of fault indictor.

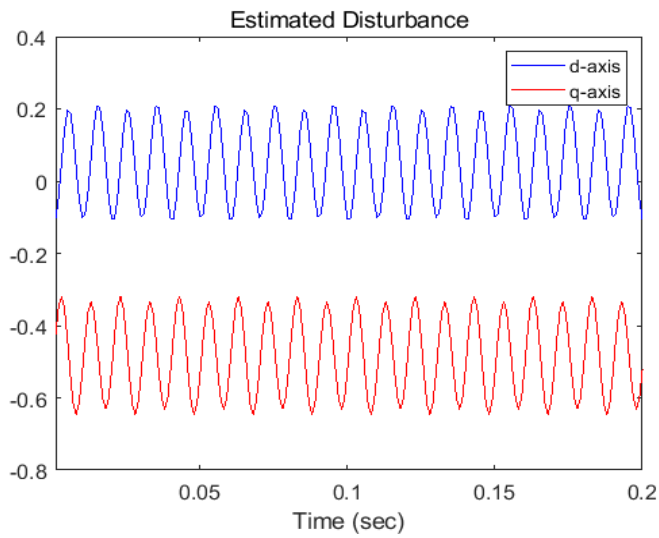

Figure 3-1 1st step of proposed method: disturbance estimation

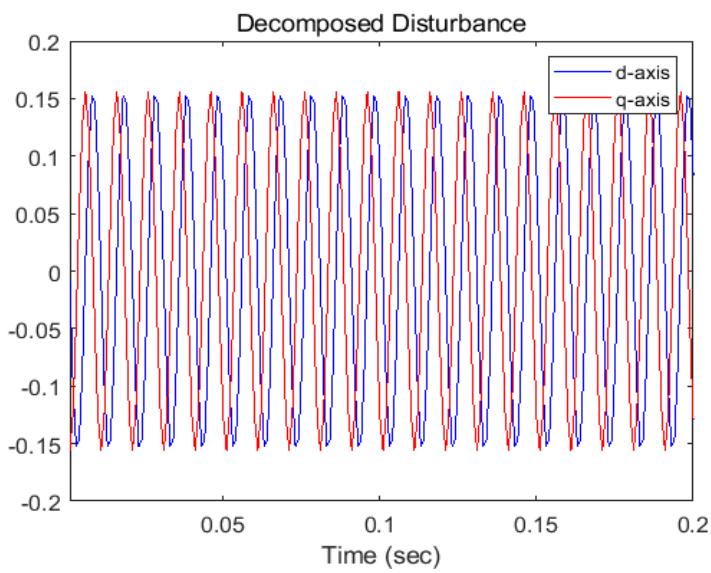

Figure 3-2 2nd step of proposed method: estimated disturbance decomposition

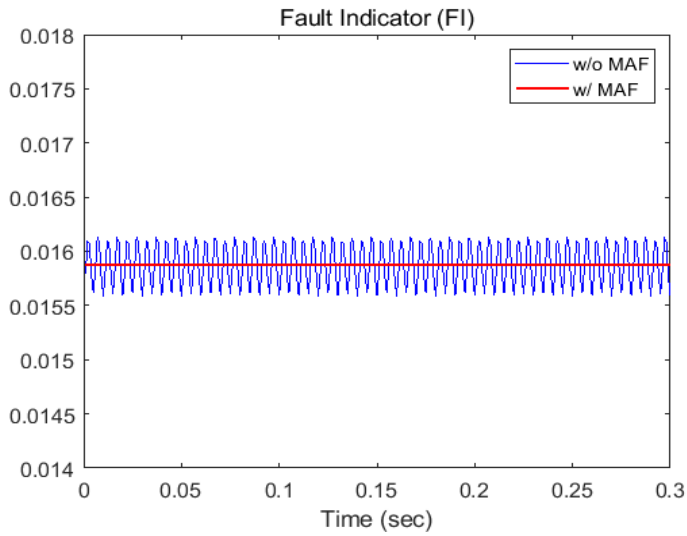

Figure 3-3 3rd step of proposed method: Calculation of fault indicator

Chapter 4. Simulation

The chapter 4 deals with simulation results of the proposed method to verify its' efficiency, performance and the robustness.

4.1 Simulation Environment

The proposed method illustrated in Figure 4-1 to diagnose fault is verified by simulation using MATLAB/Simulink. Because the simulation is controlled by maximum torque per ampere (MTPA) strategy and the target motor is SPMSM, the command current i_d^* is set to zero. The specification of PMSM used in this paper is illustrated in the Table 2. The simulation is performed at various fault severity with rated load torque; μ=1~5%, R_f =0.5R_s ~ 5R_s, T_L=4.77Nm. This section shows the simulation results with various fault severity under situations; sudden fault occurrence, varying rotating speed, with parameter variations and noise.

Table 2 Specifications of the target motor

L_d	*3.3 mH*
L_q	*3.3 mH*
R_s	*0.41Ω*
P/2	*3 Pole pairs*
ψ_f	*0.066 Wb*
J	*748kg ·mm²*
Rated torque	*4.77 Nm*

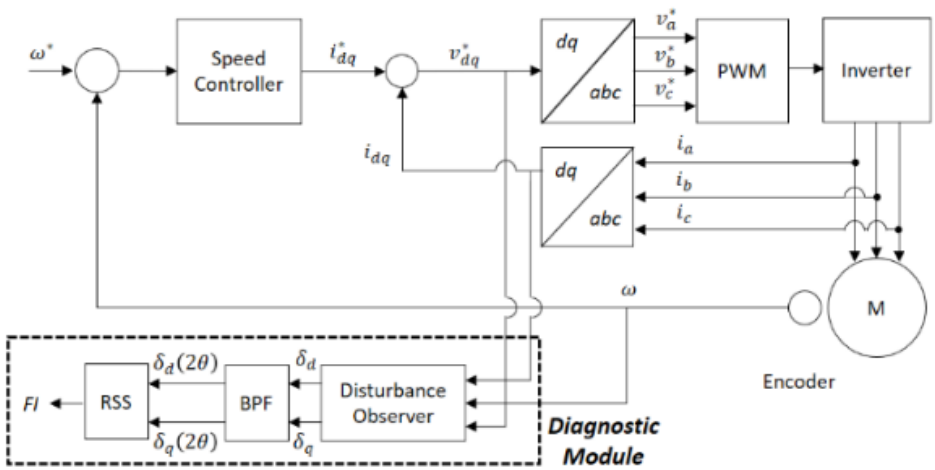

Figure 4-1 Block diagram of proposed diagnostic module

4.2 Simulation Results

Section 4.2 deals with steady-state response under sudden fault occurrence, transient response under varying rotating speed condition, the value of fault indicator with respect to various level of μ and R_f, the effect of parameter variations and the effect of unmodeled dynamics.

Figure 4-2 and Figure 4-3 shows the steady-state response and transient response of fault indicator. Figure 4-2 shows the waveform of rotating speed and fault indicator when a sudden inter-turn short-circuit fault (μ=2%, R_f =0.5R_s) occurs at t=2sec under the steady state operating condition with 1000rpm rotating speed. After the mild severity level of inter-turn short-circuit fault occurs, it seems that the motor runs without any problem because there is no noticeable change in the rotating speed. However, the proposed fault indicator rapidly increases and indicates the severity of short-circuit fault. This simulation result shows that even though the fault severity is mild, which does not interfere with operation of the motor, the proposed method is able to detect the inter-turn short-circuit fault well.

The transient response of fault indicator with inter-turn short-circuit fault (μ = 2%, R_f = *0.5*R_s) varying rotating speed is shown in Figure 4-3. In this result, the rotating speed increases in the form of a step function from 900rpm to 1100rpm. There is a surge of fault indicator for a moment when the rotating speed is changed rapidly, then it converges to the value as before. From the results, it is clear that the effect of the rotating speed condition is eliminated well. Even if the rotating speed conditions are different, the inter-turn short-circuit fault can be diagnosed regardless of the rotating speed since the values of fault indicator are the same at the same fault severity level.

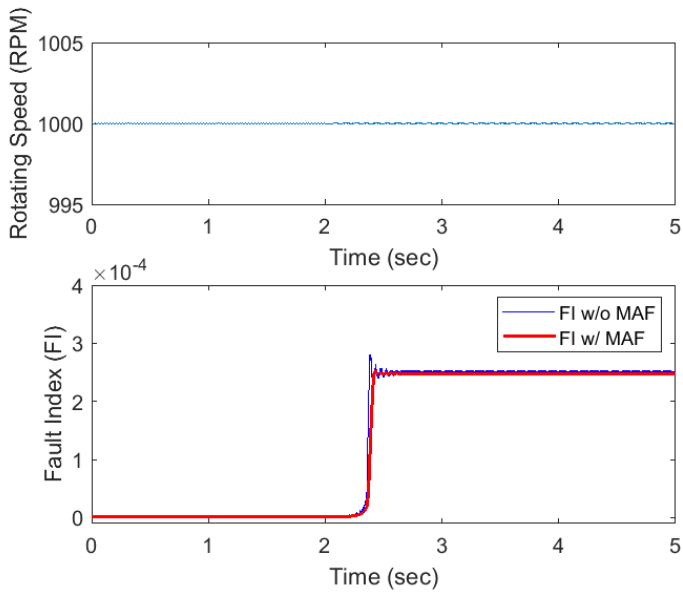

Figure 4-2 Fault indicator with sudden fault

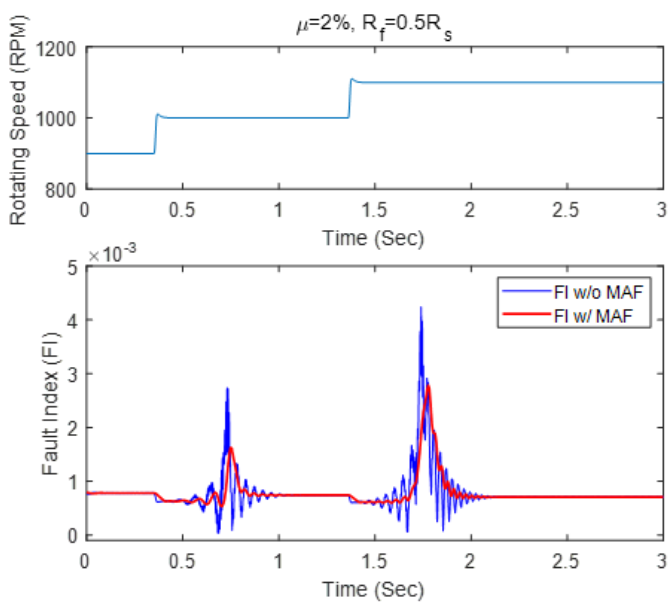

Figure 4-3 Transient response of fault indicator

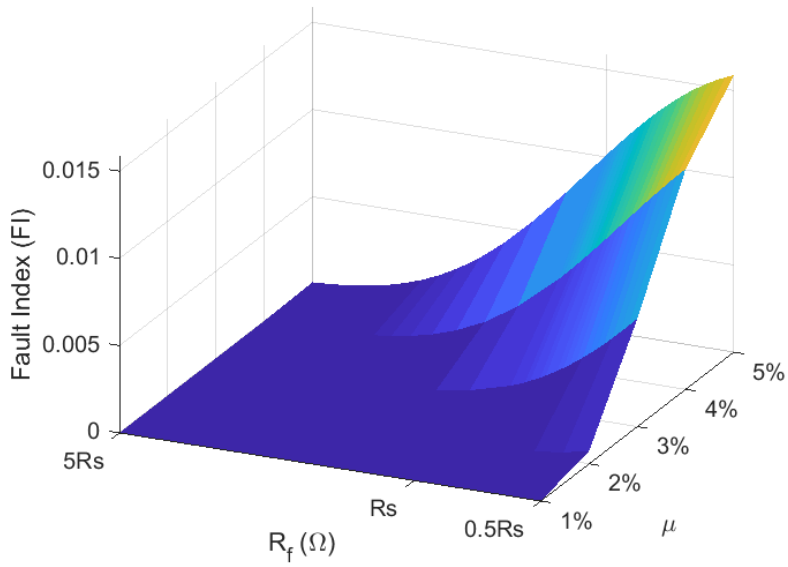

(a)

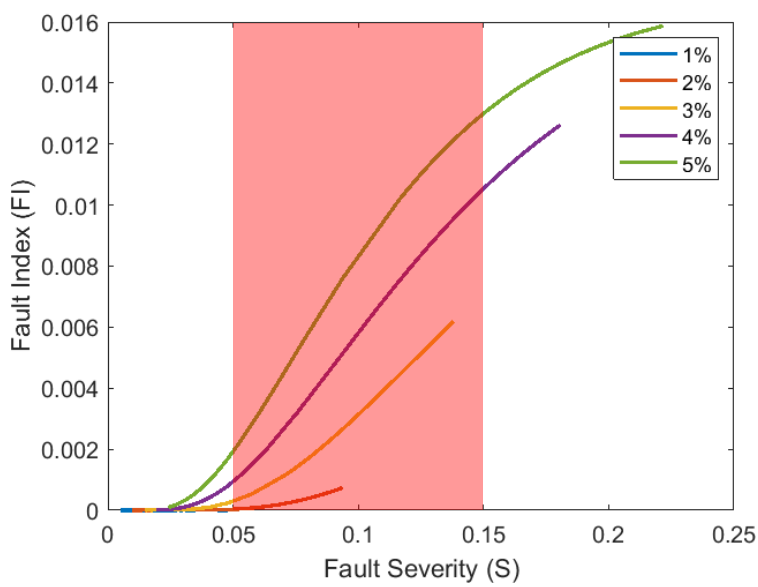

(b)

Figure 4-4 Fault indicator with respect to (a) μ (b) fault severity S

Figure 4-4 shows the value of fault indicator with respect to various fault severity. The fault indicator with respect to μ and R_f is represented in Figure 4-4(a). And Figure 4-4(b) shows the fault indicator with respect to fault severity S. As shown in the Figure 4-4, the fault indicator is a monotonically increasing function of S. Especially, inside the red box ($0.05 < S < 0.15$) the fault indicator is proportional to the fault severity level S. Therefore, the fault indicator is able to not only detect the fault but also estimate the fault severity. However, when the fault severity level is too small, fault indicator has low the sensitivity because the fault severity.

The robustness to parameter variations and unmodeled dynamics are shown in Figure 4-5 and Figure 4-6. Figure 4-5 shows the results with parameter variations ($\Delta L_s = 20\%$ and $\Delta R_s = 10\%$) with respect to μ and R_f. The Figure 4-5(b) shows the same result with respect to the value of fault indicator with and without parameter variations. From the Figure 4-5(a) and Figure 4-5(b), there is only little difference between them. Figure 4-6 shows the results with noise which is SNR = 20dB. Despite the noise, the difference between the values of fault indicator is little. Hence, it can be concluded that the proposed method is robust to the parameter variations and noise.

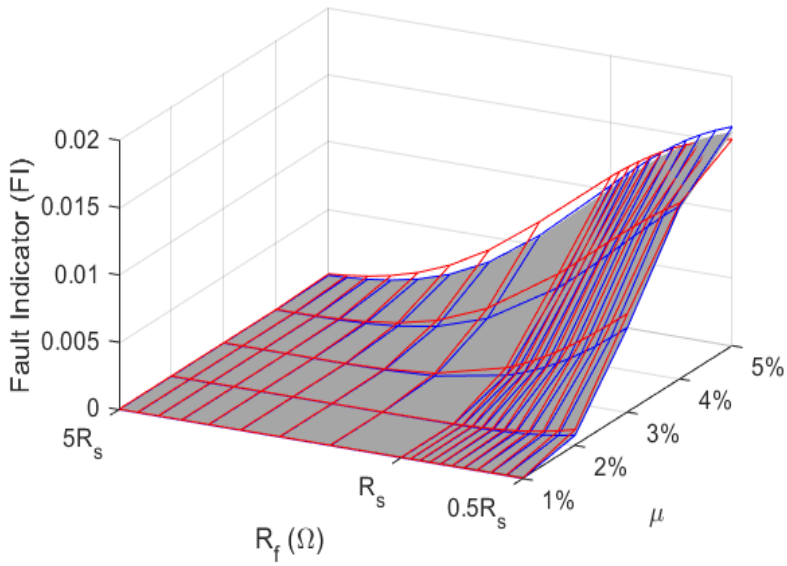

(a)

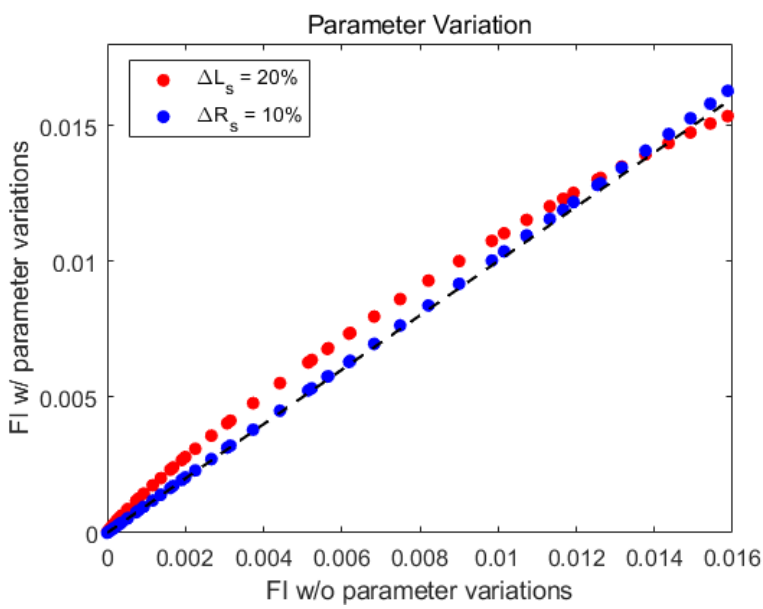

(b)

Figure 4-5 Fault indicator with parameter variations

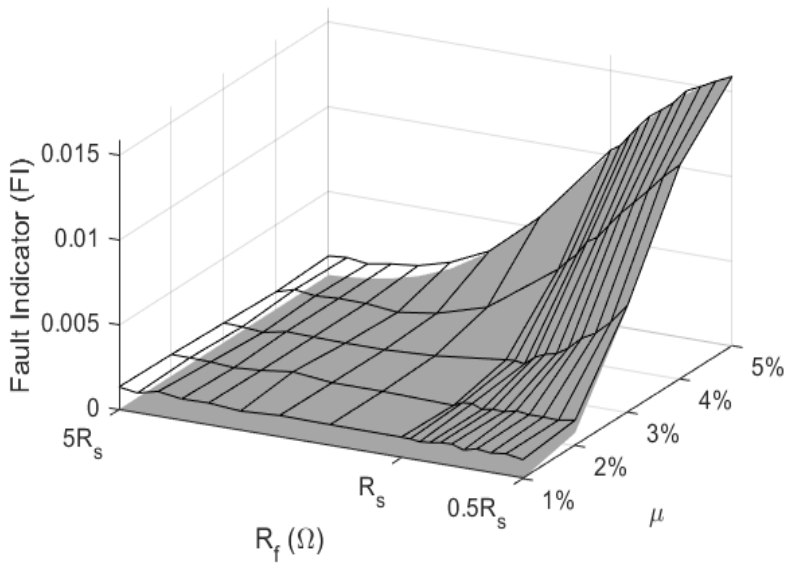

(a)

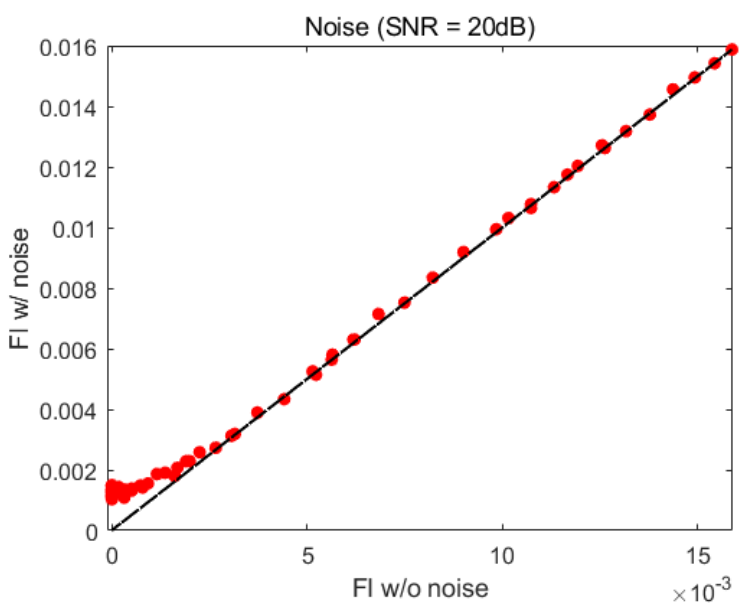

(b)

Figure 4-6 Fault indicator with noise

Chapter 5. Conclusion and Future Work

5.1 Conclusion

This thesis has proposed a method to detect an inter-turn short circuit by estimated disturbance decomposition. The proposed method consists of 3 steps; 1) The disturbance is estimated using a disturbance observer. 2) The 2^{nd} harmonic component of estimated disturbance is decomposed from the total estimated disturbance. The estimated disturbance is separated into a healthy disturbance term and a faulty disturbance term. The faulty disturbance tem of the estimated disturbance is further decomposed into two components; the DC component and the 2^{nd} harmonic component. The 2^{nd} harmonic component is appropriate to detect the fault because it is affected by only the fault of PMSM. A BPF is adopted to decompose 2^{nd} harmonic. 3) The fault indicator is calculated using 2^{nd} harmonic component of the disturbance and rotating speed. To prevent false alarm and effect of rotating speed, a new fault indicator is proposed. And lastly, a MAF is adopted to extract the DC component of the fault indicator.

The performance of proposed method has been validated by MATLAB/Simulink simulation results in terms of steady-state response, transient response, the effect of the presence of noise and the effect of the presence of parameter variations. The proposed method shows sensitivity and robustness of the fault diagnosis performance. Also it can detect inter-turn short-circuit faults without additional sensors. These strengths can facilitate on-line fault diagnosis in industrial field applications under complex operating environments.

5.2 Future Work

Although the proposed method successfully diagnoses the fault, there is a point to be supplemented in this research. The proposed method is only validated by MATLAB/Simulink simulation results and experimental verification has not been performed. To facilitate this proposed technology to practical industrial application, the experiment to validate its' performance and availability should be performed.

Bibliography

[1] J. Hang, J. Zhang, M. Cheng, and J. Huang, "Online Interturn Fault Diagnosis of Permanent Magnet Synchronous Machine Using Zero-Sequence Components," *IEEE Transactions on Power Electronics,* vol. 30, no. 12, pp. 6731-6741, 2015.

[2] P. Albrecht, J. Appiarius, R. McCoy, E. Owen, and D. J. I. t. o. E. C. Sharma, "Assessment of the reliability of motors in utility applications-Updated," no. 1, pp. 39-46, 1986.

[3] B.-J. Sung and J.-B. J. J. o. I. C. o. E. E. Lee, "Reliability improvement of machine tool changing servo motor," vol. 1, no. 1, pp. 28-32, 2011.

[4] E. L. Bonaldi, L. E. d. L. de Oliveira, J. G. B. da Silva, G. Lambert-Torresm, and L. E. B. da Silva, "Predictive maintenance by electrical signature analysis to induction motors," in *Induction Motors-Modelling and Control*: InTech, 2012.

[5] J. Yang, S. B. Lee, J. Yoo, S. Lee, Y. Oh, and C. J. I. T. o. P. E. Choi, "A stator winding insulation condition monitoring technique for inverter-fed machines," vol. 22, no. 5, pp. 2026-2033, 2007.

[6] J.-K. Park and J. J. I. T. o. I. E. Hur, "Detection of inter-turn and dynamic eccentricity faults using stator current frequency pattern in IPM-type BLDC motors," vol. 63, no. 3, pp. 1771-1780, 2015.

[7] M. A. S. Khan and M. A. J. I. T. o. I. E. Rahman, "Development and implementation of a novel fault diagnostic and protection technique for IPM motor drives," vol. 56, no. 1, pp. 85-92, 2008.

[8] A. G. Espinosa, J. A. Rosero, J. Cusido, L. Romeral, and J. A. J. I. T. o. E. C. Ortega, "Fault detection by means of Hilbert–Huang transform of the stator current in a PMSM with demagnetization," vol. 25, no. 2, pp. 312-318, 2010.

[9] L. Romeral, J. C. Urresty, J.-R. R. Ruiz, and A. G. J. I. T. o. I. E. Espinosa, "Modeling of surface-mounted permanent magnet synchronous motors with stator winding interturn faults," vol. 58, no. 5, pp. 1576-1585, 2010.

[10] R. Hu, J. Wang, A. R. Mills, E. Chong, and Z. J. I. T. o. P. E. Sun, "Detection and Classification of Turn Fault and High Resistance Connection Fault in Permanent Magnet Machines based on Zero Sequence voltage," 2019.

[11] M. A. Mazzoletti, G. R. Bossio, C. H. De Angelo, and D. R. J. I. T. o. I. E. Espinoza-Trejo, "A model-based strategy for interturn short-circuit fault diagnosis in PMSM," vol. 64, no. 9, pp. 7218-7228, 2017.

[12] J. Arellano-Padilla, M. Sumner, and C. J. I. E. p. a. Gerada, "Winding condition monitoring scheme for a permanent magnet machine using high-frequency injection," vol. 5, no. 1, pp. 89-99, 2011.

[13] G. Wang, L. Yang, G. Zhang, X. Zhang, and D. J. I. T. o. P. E. Xu, "Comparative investigation of pseudorandom high-frequency signal injection schemes for sensorless IPMSM drives," vol. 32, no. 3, pp. 2123-2132, 2016.

[14] A. Guezmil *et al.*, "Detecting inter-turn short-circuit fault in induction machine using high-order sliding mode observer: simulation and experimental verification," vol. 28, no. 4, pp. 532-540, 2017.

[15] J.-C. Urresty, J.-R. Riba, and L. J. I. T. o. P. E. Romeral, "Diagnosis of interturn faults in PMSMs operating under nonstationary conditions by applying order tracking filtering," vol. 28, no. 1, pp. 507-515, 2012.

[16] Y. Deng, J. Wang, H. Li, J. Liu, and D. J. I. t. Tian, "Adaptive sliding mode current control with sliding mode disturbance observer for PMSM drives," vol. 88, pp. 113-126, 2019.

[17] Y. A.-R. I. J. I. t. o. i. e. Mohamed, "Design and implementation of a robust current-

control scheme for a PMSM vector drive with a simple adaptive disturbance observer," vol. 54, no. 4, pp. 1981-1988, 2007.

[18] X. Liu, H. Yu, J. Yu, and L. J. I. A. Zhao, "Combined speed and current terminal sliding mode control with nonlinear disturbance observer for PMSM drive," vol. 6, pp. 29594-29601, 2018.

국문 초록

본 논문에서는 추정 외란 신호 분리 기법을 이용한 표면부착형 영구자석 전동기의 권선 단락 고장 진단 기법을 제안한다. 제안하는 방법은 총 세 단계로 이루어져 있다. 첫 번째 단계는 외란 관측기를 사용해 전동기의 전체 외란 신호를 추정하는 단계이다. 두 번째 단계는 추정한 외란 신호를 분리하는 단계이다. 외란 신호는 모델 불확실성으로 인한 정상 외란과 고장으로 인한 고장 외란으로 구성되는데, 고장 외란은 다시 직류 신호와 2차 고조파 신호로 구성된다. 직류 외란 신호는 파라미터 변동에 크게 영향을 받는 반면, 2차 고조파는 권선 단락 고장에 의해서만 영향을 받기 때문에 이 단계에서는 대역통과필터를 사용해 추정 외란 신호로부터 2차 고조파를 분리해낸다. 마지막 단계는 분리해낸 2차 고조파를 이용해 본 연구에서 새롭게 제시하는 Fault indicator를 계산하고 이동 평균 필터를 통해 그 직류 성분을 분리한다. 세 단계를 거친 Fault indicator 값은 고장 심각도에 비례하는 거동을 보임으로써 고장을 진단할 수 있을 뿐만 아니라 고장 심각도를 추정할 수 있다. 제안하는 방법은 시뮬레이션을 통해 정상 응답, 과도 응답, 강건성 그리고 다양한 고장 심각도 하에서 검증되었다. 파라미터 변동과 노이즈 등 모델 불확실성에 강건하며 외부의 추가적인 센서가 필요하지 않다는 점에서 복잡한 작동 환경의 설비에 적용이 용이할 것으로 보인다.

주요어: 고장 진단
권선 단락 고장
영구자석 동기 전동기
외란 관측기

학 번: 2018-22822